Journal of Radiation Research, Vol. 58, No. 1, 2017, pp. 33–40
doi: 10.1093/jrr/rrw083
Advance Access Publication: 10 September 2016

Analysis of liver damage from radon, X-ray, or alcohol treatments in mice using a self-organizing map

Norie Kanzaki[1], Takahiro Kataoka[1], Reo Etani[1], Kaori Sasaoka[1], Akihiro Kanagawa[2] and Kiyonori Yamaoka[1*]

[1]Graduate School of Health Sciences, Okayama University, 5-1 Shikatacho, 2-chome, Kita-ku, Okayama-shi, Okayama 700-8558, Japan
[2]Faculty of Computer Science and System Engineering, Okayama Prefectural University, 111 Kuboki, Soja-shi, Okayama 719-1197, Japan
*Corresponding author. Graduate School of Health Sciences, Okayama University, 5-1 Shikata-cho, 2-chome, Kita-ku, Okayama-shi, Okayama 700-8558, Japan. Tel/Fax: +81-86-235-6852; Email: yamaoka@md.okayama-u.ac.jp
Received April 27, 2016; Revised June 24, 2016; Accepted June 30, 2016

ABSTRACT

In our previous studies, we found that low-dose radiation inhibits oxidative stress–induced diseases due to increased antioxidants. Although these effects of low-dose radiation were demonstrated, further research was needed to clarify the effects. However, the analysis of oxidative stress is challenging, especially that of low levels of oxidative stress, because antioxidative substances are intricately involved. Thus, we proposed an approach for analysing oxidative liver damage via use of a self-organizing map (SOM)—a novel and comprehensive technique for evaluating hepatic and antioxidative function. Mice were treated with radon inhalation, irradiated with X-rays, or subjected to intraperitoneal injection of alcohol. We evaluated the oxidative damage levels in the liver from the SOM results for hepatic function and antioxidative substances. The results showed that the effects of low-dose irradiation (radon inhalation at a concentration of up to 2000 Bq/m^3, or X-irradiation at a dose of up to 2.0 Gy) were comparable with the effect of alcohol administration at 0.5 g/kg bodyweight. Analysis using the SOM to discriminate small changes was made possible by its ability to 'learn' to adapt to unexpected changes. Moreover, when using a spherical SOM, the method comprehensively examined liver damage by radon, X-ray, and alcohol. We found that the types of liver damage caused by radon, X-rays, and alcohol have different characteristics. Therefore, our approaches would be useful as a method for evaluating oxidative liver damage caused by radon, X-rays and alcohol.

KEYWORDS: liver damage, oxidative stress, self-organizing map, radon, X-ray, alcohol

INTRODUCTION

Animals, including humans, have a defence system against oxidative stress, and antioxidants play an important role in inhibiting the accumulation of reactive oxygen species (ROS) generated from oxidative stress [1]. It is well known that oxidative stress is induced by various lifestyle-related factors, such as exposure to radiation [2], heavy drinking [3–5], smoking [6, 7], a poor diet [8], and aging [9, 10]. The metabolism of alcohol in the liver follows three pathways: the alcohol dehydrogenase, microsomal ethanol oxidation, and catalase pathways. Each of these pathways produce ROS, including superoxide anion radicals (O_2^-), hydroxyl radicals ($^-$OH), and hydrogen peroxide (H_2O_2) [3]. Moreover, irradiation also generates ROS, either directly or indirectly [2]. It has been recognized that the ROS produced by these factors are involved with cancer, inflammatory immune injury, and so on [1]. On the other hand, we have reported that low-dose irradiation inhibits oxidative stress–induced diseases in the mouse liver due to the consequent increases in antioxidative substances, including superoxide dismutase (SOD), catalase (Cat), glutathione peroxidase (GPx), glutathione (GSH) and glutathione reductase (GR) [11–13].

A self-organizing map (SOM) is an unsupervised neural network algorithm that models the ability of a neuron to handle information

in the primary visual area [14]. Multidimensional data are summarized in a map by data compression during the learning process. A SOM can be used to find clusters in the input data in order to identify unknown data and extract new knowledge. It has been proven useful in complex analyses of biochemical data, such as in determining gene expression patterns [15–17] and for diagnostic assistance [18, 19]. However, there are no reports comparing the different effects of oxidative stress caused by the various factors.

Since the 2011 nuclear accident in Fukushima, the health effects of low-dose irradiation have been at the forefront of public attention. A high priority for medical research is to provide accurate information on radiation health effects to the public. We have attempted to quantify oxidative damage after low-dose irradiation. We have previously demonstrated that radon inhalation has antioxidative effects in the mouse liver, and that the inhibitory effects of radon inhalation at a concentration of 2000 Bq/m^3 on carbon tetrachloride–induced hepatopathy are almost equivalent to those of treatment with ascorbic acid at a dose of 500 mg/kg or α-tocopherol at 300 mg/kg [20]. We have quantitatively shown the positive effects of radon inhalation; however, further analysis of the effects of irradiation is needed.

The inhibitaion of oxidative stress following low-dose radiation has been controversial. The objective of this study was to compare radiation-induced liver damage with alcohol-induced liver damage. Here, we used a SOM for the analysis because it is a useful tool for the visualization of oxidative damage induced by different sources. To determine the antioxidative function, we focused on the changes in antioxidants (such as SOD, GSH and Cat) in a mouse liver, and the hepatic function parameters in serums [such as glutamic oxaloacetic transaminase (GOT) and glutamic pyruvic transaminase (GPT)] after irradiation or alcohol administration. We also analyzed oxidative liver damage caused by radon, X-rays or alcohol by using a SOM.

MATERIALS AND METHODS

Animals

C57BL/6J mice (age, 8 weeks; sex, male; bodyweight, 21–28 g) were obtained from Charles River (Yokohama, Japan). All experimental protocols in this study were approved by the Animal Experimentation Committee of Okayama University. The mice were housed under a 12:12 h artificial light cycle (8:00 a.m. to 8:00 p.m.) and were divided into 12 groups: radon-inhaling groups (sham, 500 Bq/m^3, 1000 Bq/m^3, 2000 Bq/m^3), X-irradiated groups (sham, 0.5 Gy, 1.0 Gy, 2.0 Gy) and 50% alcohol-administered groups (sham, 0.5 g/kg, 2.0 g/kg, 5.0 g/kg).

Radon inhalation

In the radon-inhaling group, we used a radon exposure system as described in a previous report [21]. To generate conditions for the inhalation of specific radon concentrations, the 'Doll Stone' radon source (Ningyotoge Genshiryoku Sangyo, Co., Ltd, Okayama, Japan) was placed in a radon tank. The radon inhalation system blows air containing radon from the tank into a mouse cage. The radon concentration in the mouse cage was controlled using the Doll Stone and measured using a radon monitor (CRM-510; femto-TECH, Inc., OH, USA). Mice inhaled radon at background level concentrations of 20 (sham), 500, 1000 or 2000 Bq/m^3 for 24 h. Mice were euthanized by deep ether anesthesia immediately after radon inhalation. Blood was collected from the heart for GOT and GPT analyses, and intact livers were quickly removed for SOD, GSH and Cat analyses.

X-ray exposure

In the X-irradiated group, the mice received whole-body irradiation at doses of 0.5 Gy, 1.0 Gy or 2.0 Gy (tube voltage, 150 kV; tube current, 20 mA; filter, 0.5 mm Al and 0.2 mm Cu; distance between focus and target, 43.5 cm) using an X-ray generator (MBR-1520R-3; Hitachi Power Solutions Co., Ltd, Ibaraki, Japan). Similar to the treatment mice, the control mice were sham-exposed. The mice were euthanized by deep ether anesthesia 4 h after X-ray exposure. Blood was collected from the heart for GOT and GPT analyses, and intact livers were quickly removed for SOD, GSH and Cat analyses.

Alcohol administration

In the alcohol-administered group, mice were treated with 50% alcohol at concentrations of 0.5, 2.0 or 5.0 g/kg bodyweight intraperitoneally. The control mice ('the sham group') were administered saline. Mice were euthanized by deep ether anesthesia 24 h after alcohol administration. Blood was collected from the heart for GOT and GPT analyses, and intact livers were quickly removed for SOD, GSH and Cat analyses.

Biochemical assays

Livers were homogenized on ice with 10 mM phosphate buffer (PBS; pH 7.4) for assays of SOD, t-GSH, Cat and protein. The homogenates were centrifuged at 12 000 × *g* for 45 min at 4°C and the supernatants were collected. Serum was collected from the supernatants by centrifuging at 3000 × *g* for 5 min for assays of GOT and GPT.

SOD activities in the livers were assayed based on the nitroblue tetrazolium (NBT) reduction method using the Wako–SOD test (Wako Pure Chemical Industry, Co., Ltd, Osaka, Japan) [22]. NBT reacts with O_2^- to form diformazan, and SOD reacts with O_2^- to form H_2O_2 and O_2. In this assay, the rate of inhibition of diformazan production by SOD was measured at 560 nm using a spectrophotometer (Viento XS; DS Pharma Biomedical Co., Ltd, Osaka, Japan). One unit of enzyme activity is defined as 50% of the inhibition rate.

The t-GSH content in the liver was assayed using the Bioxytech GSH-420 assay kit (OXIS Health Products, Inc., Portland, OR, USA). Tissue samples from the liver were mixed with trichloroacetic acid solution. The solutions were centrifuged at 3000 × *g* for 10 min at 4°C and the upper aqueous layers were collected. This method is based on the formation of a chromophoric thione. The absorbance measured at 420 nm using a spectrophotometer is directly proportional to the GSH concentration.

Cat activity in the livers was assayed from the H_2O_2 reduction rate at 37°C [23]. Briefly, 20 µl of the supernatant of the liver homogenate were mixed with 50 µl of 1 M Tris-HCl buffer containing

5 mM ethylenediaminetetraacetic acid (pH 7.4), 900 µl of 10 mM H_2O_2 and 30 µl of deionized water. The changes in absorbance were monitored for 1 min. Cat activity was calculated using a molar extinction coefficient of 7.1×10^{-3} $M^{-1}cm^{-1}$.

GOT and GPT activities in the serum were assayed based on the pyruvate oxidase-N-ethyl-N-(2-hydroxy-3-sulfopropyl)-m-toluidine (POP-TOOS) method using the Transaminase CII-Test Wako (Wako Pure Chemical Industry, Co., Ltd, Osaka, Japan).

The protein content in each sample was measured by the Bradford method [24] using the Protein Quantification Kit-Rapid (Dojindo Molecular Technologies, Inc., Kumamoto, Japan).

Statistical analyses

The results are presented as the mean ± standard error of the mean (SEM). Significant differences between the sham group and treated groups were analyzed by ANOVA and Dunnett's test.

SOM

A SOM [14] has an input layer and an output layer with associated weights (Fig. 1). It constructs an output map from multidimensional input data by learning. We optimized the initial randomized map via machine learning of the input data. Briefly, the SOM found the best matching unit (BMU) closest to the input data by searching the minimum value of the distance between the input data and each of the units in the output map. The characteristics of the input data were reflected in the neighborhood of the BMU. We repeatedly updated the output map. We were able to receive information from the output map because the SOM places data with similar patterns into similar locations.

We analyzed oxidative liver damage using SOM PAK (SOM Programming Team of the Helsinki University of Technology Laboratory of Computer and Information Science, Espoo, Finland) and Blossom (SOM Japan, Co. Ltd, Tottori, Japan). The results of the biochemical assay were normalized using the following formula: $x = x'/AVE_{Sham}$, where, x' is the value of SOD, GSH, Cat, GOT and GPT, and AVE_{Sham} is the average of the sham groups (radon, X-ray or alcohol). Therefore, the average of x in each sham group was normalized (SOD, GSH, Cat, GOT, GPT) = (1, 1, 1, 1, 1) as the control standard.

SOM PAK is a 2D map and Blossom is a spherical map. In Experiment 1, SOM PAK was used to present liver damage by radiation, such as by radon and X-ray, on a map that summarized the data for the alcohol-induced liver damage, as 2D maps pointing out valuable information. Briefly, the SOM learned the data in the alcohol-administered group and constructed the output maps. Subsequently, the BMUs of the radon-inhaled groups (sham, 500 Bq/m^3, 1000 Bq/m^3 or 2000 Bq/m^3) and X-irradiated groups (sham, 0.5 Gy, 1.0 Gy or 2.0 Gy) were calculated. Finally, we mapped the relationship between the radiation-induced liver damage and the alcohol-induced liver damage. In this experiment, the width of the output map, the height of the output map, the number of learnings, the learning rate, and the radius of the neighborhood are 60 units, 40 units, 100 000 steps, 0.02, and 15 units, respectively. In Experiment 2, Blossom was used for establishing the liver damage caused by the various factors, such as radon, X-rays and alcohol, because spherical maps make it easier to consider the relationship of many clusters. Some configurations are automatically and optimally set. Clustering was applied according to the results from Blossom.

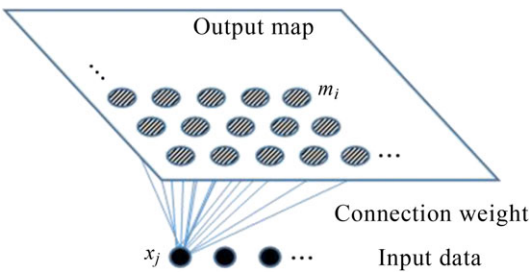

Fig. 1. Structure of a self-organizing map (SOM). m_i is *i*th unit in output map. x_i is *j*th input data.

RESULTS

Evaluation of liver damage by radon, X-rays or alcohol by using statistical analysis

We first statistically analyzed the changes in the parameters of hepatic function (Fig. 2). GOT activity in the 2000 Bq/m^3 radon–inhaling group was significantly lower than that in sham-inhaling group. GPT activity in the 1.0 Gy X-irradiated group was significantly higher than that in sham-irradiated group. GOT activity in the 5.0 g/kg alcohol–administered group was significantly higher than that in the sham-administered group. GPT activity in the 5.0 g/kg alcohol–administered group was significantly higher than that in the sham-irradiated group.

Next, we statistically analyzed the changes in the parameters of antioxidative function due to evaluation of oxidative damage in liver (Fig. 3). Radon inhalation did not change any antioxidative substances. In the X-irradiated group, although no significant changes were observed in Cat activity, 0.5, 1.0 and 2.0 Gy irradiation significantly increased SOD activity. Similarly, 2.0 Gy irradiation significantly increased GSH content. In the alcohol-administered group, although no significant changes were observed in Cat activity, SOD activity in the 5.0 g/kg bodyweight alcohol–administered group was significantly lower than that in the sham-administered group. GSH content in the 5.0 g/kg bodyweight alcohol–administered group was significantly lower than that in the sham-administered group.

Evaluation of liver damage by radon, X-rays or alcohol by using a SOM

Experiment 1

We constructed an output map that learned the effect of alcohol administration on the liver (Fig. 4). The 5.0 g/kg bodyweight alcohol–administered group was put on the left half of the output map, and the other groups and control standard (SOD, GSH, Cat, GOT, GPT) = (1, 1, 1, 1, 1), were discretely put on the right half of the output map. The 5.0 g/kg bodyweight alcohol–administered group was sharply distinguished from the other groups. However, the 2.0 g/kg bodyweight and 0.5 g/kg bodyweight alcohol–administered groups were less sharply distinguished. Specifically, the 2.0 g/kg bodyweight alcohol–administered group was put on the upper right

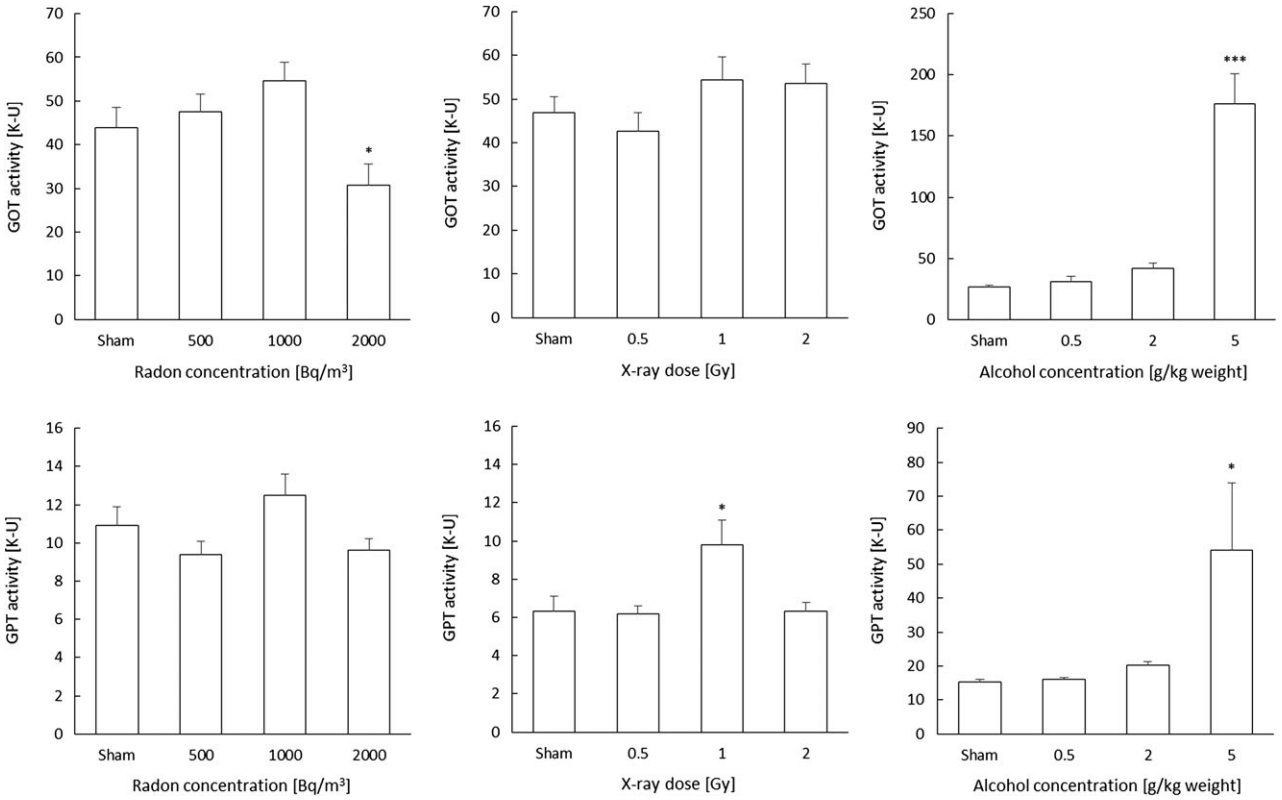

Fig. 2. Changes in GOT and GPT activity in liver following exposure to radon, X-rays or alcohol. Number of mice per experimental point was six. *$P < 0.05$, **$P < 0.01$, ***$P < 0.001$ vs sham in each group.

of the output map and the 0.5 g/kg bodyweight alcohol–administered group was put on the lower right of the output map. Thus, the output map was able to show a summarizing assessment of liver damage.

Finally, we calculated liver damage by radiation, such as from radon and X-rays (Fig. 4). All of the radon-inhaling and X-irradiated groups were put on the lower right of the above-mentioned output map. The data indicated that the radon-inhaling and X-irradiated groups were of similar levels to the 0.5 g/kg bodyweight alcohol–administered group.

Experiment 2

We analyzed liver damage by various factors (such as radon, X-rays or alcohol) using Blossom (Fig. 5). Similar to Experiment 1, the 5.0 g/kg bodyweight alcohol–administered group was sharply distinguished from the other groups. The other groups were less clearly distinguished based on the results of Experimental 2. Although not all of the data was classified properly, we found interesting characteristics from a dendrogram (Fig. 6). The alcohol-administered group and X-irradiated group were large classifications based on the results of Experimental 2. Moreover, the data in the alcohol-administered group was classified into four subgroups based on the level of liver damage. These findings showed that a spherical SOM could express the effects of alcohol-induced liver damage. The data in the X-irradiated group had no conspicuous subclassification. This result indicated that there were no changes between the 0.5 and 2.0 Gy administrations.

Hence, alcohol-induced liver damage had characteristics that were different from liver damage by X-rays. We concluded that liver damage caused by radon at concentrations of up to 2000 Bq/m^3 would be similar to that caused by 0.5 g/kg bodyweight alcohol administration, because the 2000 Bq/m^3 radon–inhaling group and the 0.5 g/kg bodyweight alcohol–administered group were classified together based on the results of Experiment 2. Likewise, we concluded that the liver damage caused by radon at a concentration of 500 Bq/m^3 was similar to that caused by an X-ray dose of up to 2.0 Gy, because the 500 Bq/m^3 radon–inhaling group and the X-irradiated group were grouped into the same class.

DISCUSSION

Alcohol-induced liver damage is primarily related to oxidative stress. It is well known that alcohol-induced liver damage sharply increases GOT and GPT in the serum, and that acute alcohol administration depletes GSH and reduces antioxidants in 24 h due to the detoxification of alcohol [13, 25]. Thus, it is expected that oxidative stress is induced 24 h after alcohol administration. On the other hand, exposure to low-dose X-rays and radon leads to the early activation of SOD. For radon exposure, it has been reported that SOD activity in the mouse liver tended to reach a peak within 24 h [26]. For X-ray exposure, although there were no changes with high-dose

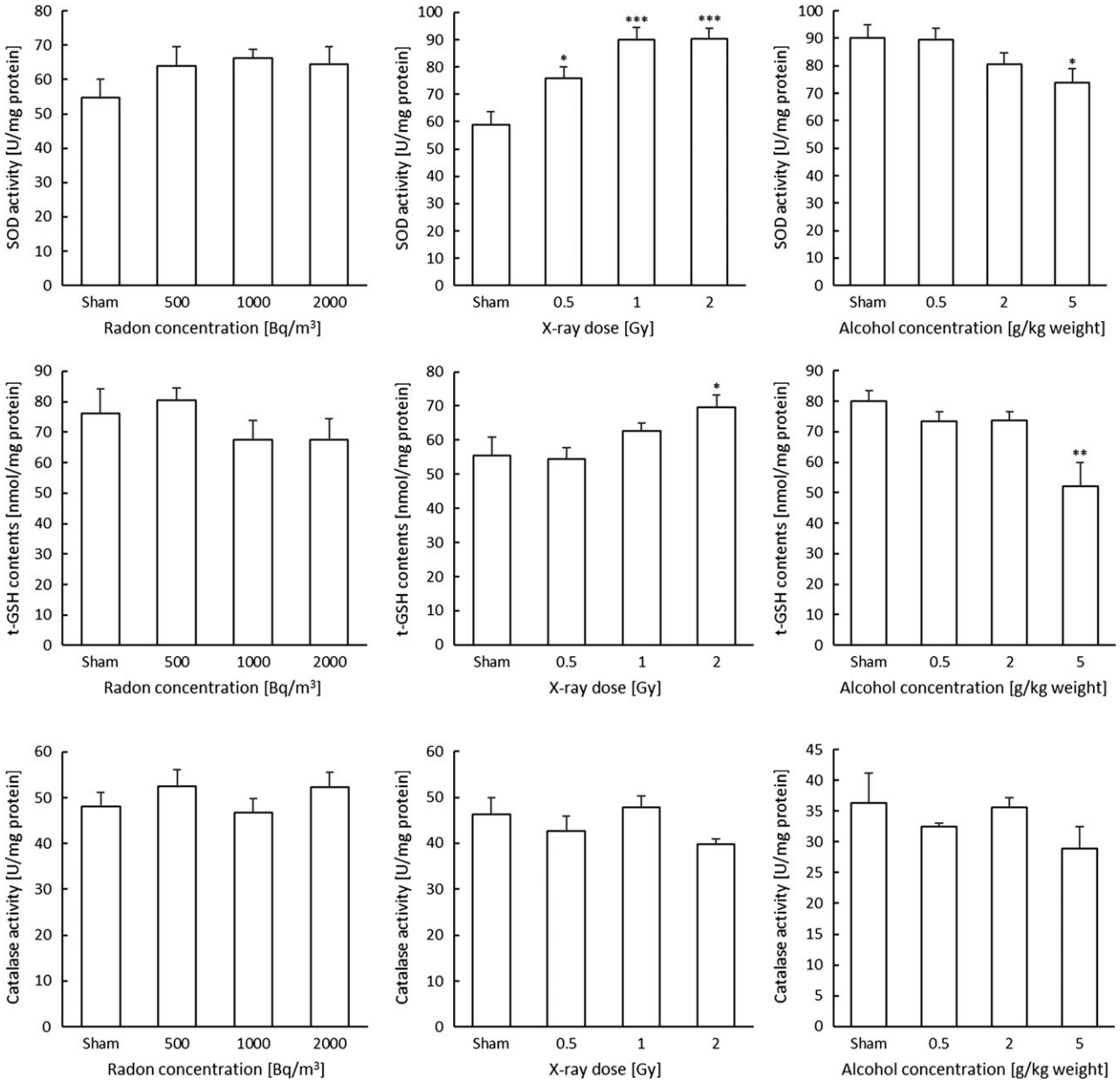

Fig. 3. Changes in SOD activity, t-GSH content, and Cat activity in liver following exposure to radon, X-rays or alcohol. Number of mice per experimental point was six. *$P < 0.05$, **$P < 0.01$, ***$P < 0.001$ vs sham.

X-rays (10 Gy), a low-dose increased SOD activities at 4 h after irradiation [27]. In this study, we analyzed the liver damage after radon inhalation for 24 h, at 4 h after X-irradiation, and at 24 h after alcohol administration. GOT and GPT activities at 5.0 g/kg bodyweight in the alcohol-administered group were significantly higher than in the sham-administered group. In addition, antioxidants, such as SOD and catalase, were significantly reduced by 5.0 g/kg bodyweight with alcohol administration. Therefore, these results suggest that the mouse livers were oxidatively damaged by alcohol administration at 5.0 g/kg bodyweight. In the other treated groups, GOT and GPT activities were not sharply increased. Although there were hardly any changes to antioxidant levels, SOD activities in the X-irradiated group and the radon-inhaling group tended to increase depending on the X-ray dose. Therefore, our results show that enhancement of antioxidative function by low-dose X-irradiation and radon inhalation was extremely small and highly individual.

As mentioned previously, the effects of low levels of oxidative stress due to irradiation and alcohol administration are uncertain because the mechanisms are complicated by the fact that oxidative stress–related substances are involved in quick chain reactions. However, it is important to analyze not only hepatic function, but also antioxidative function to verify liver damage. We have validated

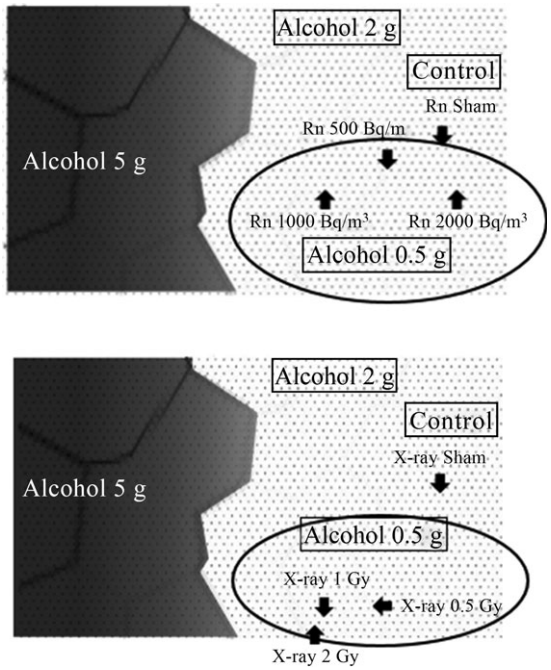

Fig. 4. Output map for analysis of liver damage by radon, X-rays or alcohol by using a self-organizing map (SOM). Calculated oxidative levels in the liver of radon-inhaled X-irradiated mice are expressed as an output map for liver damage by alcohol groups. Sources of similar oxidative levels are located in the same area (mild oxidative stress, white area; severe oxidative stress, gray area).

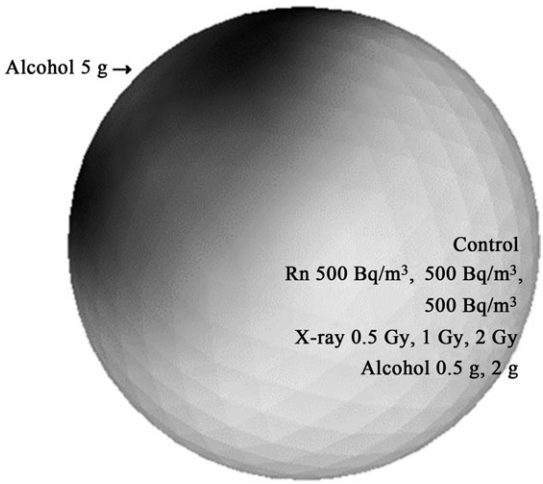

Fig. 5. Output map for analysis of liver damage by radon, X-rays or alcohol by using a spherical self-organizing map (SOM). Sources of similar oxidative levels are located in the same area (mild oxidative stress, white area; severe oxidative stress, gray area). The spherical SOM shows two clusters divided between 5.0 g/kg bodyweight alcohol-administered group and the other groups.

diagnoses of hepatitis using a SOM [19]. In the present study, we attempted to analyze the more difficult fuzzy clustering caused by liver damage from low oxidative stress. Thus, we proposed that oxidative liver damage is best visualized by an overall assessment of changes in hepatic function and antioxidant levels using a SOM. Specifically, we obtained new knowledge from the output map by the SOM. As SOMs place data with similar patterns onto similar locations, liver damage by radon inhalation (at a concentration of up to 2000 Bq/m^3) and X-ray irradiation (at a dose of up to 2.0 Gy) were considered similar to that caused by alcohol at 0.5 g/kg bodyweight administration because of their placement on the map. We found that it was easy to compare liver damage due to different factors. Moreover, we applied a spherical SOM to analyze oxidative liver damage. Ritter proposed that the spherical form would be more suitable as a structure of SOMs [28]. Some problems of boundary effect information conveying and computing speed have been solved by spherical SOMs [29, 30]. Thus, we showed a comparison of liver damage due to radon, X-rays and alcohol using a spherical SOM. The spherical SOM adapted characteristics and made seamless changes through a comprehensive evaluation of liver damage. Although we obtained no evidence of specific characteristic oxidative stress caused by radon inhalation, the X-irradiated and alcohol-administered groups were sharply divided in the dendrogram based on the output map of the spherical SOM. We discovered the different patterns of liver damage caused by different factors. The radon-inhaling group and X-irradiated groups were categorized into the same group as the control group or the 0.5 g/kg bodyweight alcohol-administered group based on the results of Experimental 2, respectively. This result was consistent with the results of the 2D SOM. Further work is needed to explore the differences in liver damage caused by the different factors.

In our previous study, we found there were differences between liver damage that was due to radon, X-ray or alcohol treatment. However, it was still unclear what exactly the differences were. We reported a radon concentration of ~3 mBq/kg in the liver of mice after continuous radon inhalation at a concentration of 1 Bq/m^3 [31]. According to our report, the absorbed dose in the liver was ~140 nGy under the experimental conditions. Although we reported that radon at a concentration of 2000 Bq/m^3 for 24 h or X-ray exposure at a dose of 0.5 Gy enhances antioxidative function, the absorbed dose of radon was much lower than that of X-ray irradiation. The results of the study also suggested that radon inhalation at a concentration of 2000 Bq/m^3 and X-irradiation at a dose of 0.5 Gy led to the same level of liver damage. Moreover, we suggested that radon inhalation at a concentration of 2000 Bq/m^3, or X-irradiation at a dose of 0.5 Gy, were comparable with the effect of alcohol administration at 0.5 g/kg bodyweight. However, we could not conclude why antioxidative functions were activated by radon inhalation in spite of the low absorbed dose. Further study was needed at this point.

Thus, in the present study, we evaluated the oxidative damage levels in the liver from the results of hepatic function and antioxidative substances by using a SOM to compare radiation-induced liver

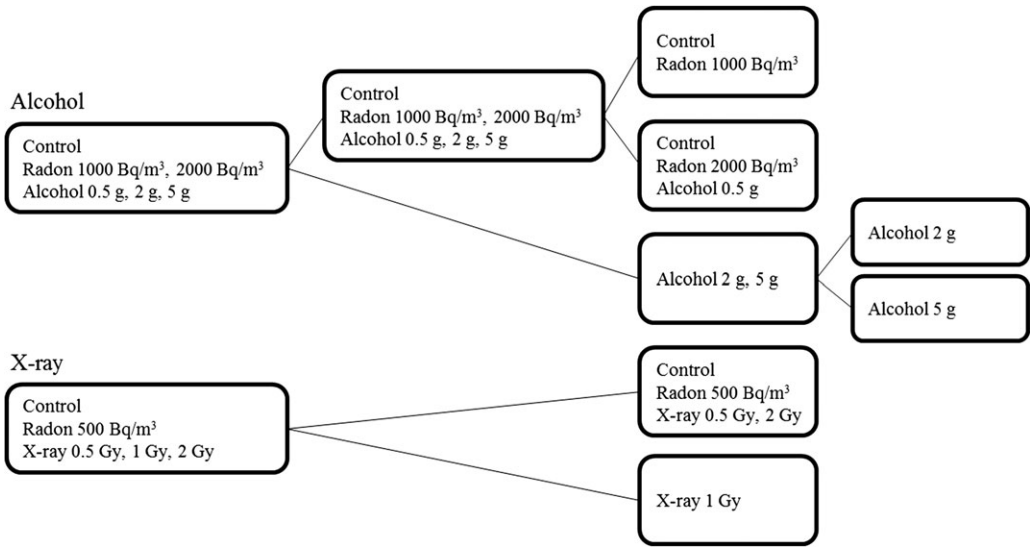

Fig. 6. Findings based on a dendrogram by a spherical self-organizing map (SOM) for classification of liver damage by radon, X-rays or alcohol.

damage with alcohol-induced liver damage. We concluded that radon inhalation at a concentration of up to 2000 Bq/m^3, or X-irradiation at a dose of up to 2.0 Gy, were comparable with the effect of alcohol administration at 0.5 g/kg bodyweight. This novel method using a SOM was successful in comprehensively examining oxidative liver damage, and our approach was useful for evaluating the oxidative stress caused by various factors. The results presented in this study provide a substantial basis for future studies aimed at elucidating the mechanisms involved in oxidative stress.

ACKNOWLEDGEMENTS

The authors thank the staff of the Departments of Animal Resources and Radiation Research at Shikata Laboratory, Advanced Science Research Center, Okayama University, for their technical support. Results from this study were presented at the International Congress of Radiation Research 2015, and Annual Meeting of Atomic Energy Scoiety of Japan 2016.

FUNDING

This work was supported by JSPS KAKENHI (Grant Number 26420872).

CONFLICT OF INTEREST

The authors state that there are no conflicts of interest.

REFERENCES

1. Riley PA. Free radicals in biology: oxidative stress and the effects of ionizing radiation. *Int J Radiat Biol* 1994;65:27–33.
2. Kumar S, Vasudevan D. Alcohol-induced oxidative stress. *Life Sci* 2007;81:177–87.
3. Wu D, Cederbaum AI. Oxidative stress and alcoholic liver disease. *Semin Liver Dis* 2009;29:141–54.
4. Albano E. Alcohol, oxidative stress and free radical damage. *Proc Nutr Soc* 2006;65:278–90.
5. Burkea A, FitzGerald GA. Oxidative stress and smoking-induced vascular injury. *Prog Cardiovasc Dis* 2003;46:79–90.
6. Van der Vaart H, Postma DS, Timens W, et al. Acute effects of cigarette smoking on inflammation and oxidative stress: a review. *Thorax* 2004;59:713–21.
7. Sies H, Stahl W, Sevanian A. Nutritional, dietary and postprandial oxidative stress. *J Nutr* 2005;135:969–72.
8. Sohal RS, Mockett RJ, Orr WC. Mechanisms of aging: an appraisal of the oxidative stress hypothesis. *Free Radic Biol Med* 2002;33:575–86.
9. Muller FL, Lustgarten MS, Jang Y, et al. Trends in oxidative aging theories. *Free Radic Biol Med* 2007;43:477–503.
10. Aruoma OI. Free radicals, oxidative stress, and antioxidants in human health and disease. *J Am Oil Chem Soc* 1998;75:199–212.
11. Yamaoka K. Activation of antioxidant system by low dose radiation and its applicable possibility for treatment of reactive oxygen species–related diseases. *J Clin Biochem Nutr* 2006;39:114–33.
12. Kataoka T. Study of antioxidative effects and anti-inflammatory effects in mice due to low-dose X-irradiation or radon inhalation. *J Radiat Res* 2013;54:587–96.
13. Toyota T, Kataoka T, Nishiyama Y, et al. Inhibitory effects of pretreatment with radon on acute alcohol-induced hepatopathy in mice. *Mediators Inflamm* 2012;2012:Article ID 382801.
14. Kohonen T. Self-organized formation of topologically correct feature maps. *Biol Cybern* 1982;43:59–69.
15. Wang J, Delabie J, Aasheim H et al. Clustering of the SOM easily reveals distinct gene expression patterns: results of a reanalysis of lymphoma study. *BMC Bioinformatics* 2002;3:36–44.
16. Törönen P, Kolehmainen M, Wong G, et al. Analysis of gene expression data using self-organizing maps. *FEBS Lett* 1999;451:142–6.

17. Sugii Y, Satoh H, Yu D, et al. Spherical self-organizing map as a helpful tool to identify category-specific cell surface markers. *Biochem Biophys Res Commun* 2008;376:414–8.
18. Kaur A, Singh N, Bahrdwaj A. A comparison of supervised multilayer back propagation and unsupervised self organizing maps for the diagnosis of thyroid disease. *Int J Comput Appl* 2013;82:39–43.
19. Kanzaki N, Kanagawa A. New method to assist discrimination of liver diseases by spherical SOM with Mahalanobis distance. *JACIII* 2011;16:55–61.
20. Kataoka T, Nishiyama Y, Yamato K, et al. Comparative study on the inhibitory effects of antioxidant vitamins and radon on carbon tetrachloride–induced hepatopathy. *J Radiat Res* 2012; 53:830–9.
21. Kataoka T, Teraoka J, Sakoda A, et al. Protective effects of radon inhalation on carrageenan-induced inflammatory paw edema in mice. *Inflammation* 2012;35:713–22.
22. Baehner R, Murrmann S, Davis J, et al. The role of superoxide anion and hydrogen peroxide in phagocytosis-associated oxidative metabolic reactions. *J Clin Investig* 1975;56:571–6.
23. Aebi H, Wyss S, Scherz B, et al. Properties of erythrocyte catalase from homozygotes and heterozygotes for Swiss-type acatalasemia. *Biochem Genet* 1976;14:791–807.
24. Bradford M. A rapid and sensitive method for the quantitation of microgram quantities of protein utilizing the principle of protein-dye binding. *Anal Biochem* 1976;72: 248–54.
25. Vogt BL, Richie JP. Glutathione depletion and recovery after acute ethanol administration in the aging mouse. *Biochem Pharmacol* 2007;73:1613–21.
26. Kataoka T, Sakoda A, Ishimori Y, et al. Study of the response of superoxide dismutase in mouse organs to radon using a new large-scale facility for exposing small animals to radon. *J Radiat Res* 2011;52:775–81.
27. Yamaoka K, Edamatsu R, Mori A. Increased SOD activities and decreased lipid peroxide levels induced by low dose X irradiation in rat organs. *Free Radic Biol Med* 1991;11:299–306.
28. Ritter H. Self-organizing maps on non-Euclidean spaces. In: Ritter H. (ed). *Kohonen Maps*. Netherlands: Elsevier, 1999, 97–108.
29. Sangole A, Knopf GK. Visualization of randomly ordered numeric data sets using spherical self-organizing feature maps. *Comput Graph* 2003;27:963–76.
30. Wu Y, Takatsuka M. Spherical self-organizing map using efficient indexed geodesic data structure. *Neural Netw* 2006;19: 900–10.
31. Sakoda A, Ishimori Y, Kawabe A, et al. Physiologically based pharmacokinetic modeling of inhaled radon to calculate absorbed doses in mice, rats, and humans. *J Nucl Sci Technol* 2010;47:731–8.